# A Vorticity-Divergence Dynamical Core based on the Nonhydrostatic Unified System of Equations on the Icosahedral Geodesic Grid

Ross Heikes, C.S. Konor and D. Randall

Dept. of Atmospheric Science
Colorado State University

Office of Science

SciDAC
Scientific Discovery through Advanced Computing

CMMAP
Reach for the sky.

# Overview

- **vorticity-divergence** dynamical core predicts the vorticity (vertical component) and divergence directly on the Z-grid (defined at cell centers).
- **unified system** is a nonhydrostatic system that is designed for global cloud resolving models which filters vertically propagating sound waves while allowing elasticity due to thermal expansion.
- **icosahedral grid**. The grid.

# Outline

1) Icosahedral grid. Grid optimization is extended to grid 12.
2) Introduction of dynamical core equations
3) Numerical results
   - Warm bubble
   - Extratropical cyclone. Jablonowski test case.
4) Conclusions and future work.

# Grid Optimization Algorithm

- The ***Voronoi Corner*** (purple dot) is defined as the point equidistant from surrounding grid points (blue dots).

- There is a flaw with the Voronoi grid -- a line connecting grid points does not bisect the cell wall.

- The algorithm positions all grid points so that red points are coincident with green points (or at least it does the best it can)

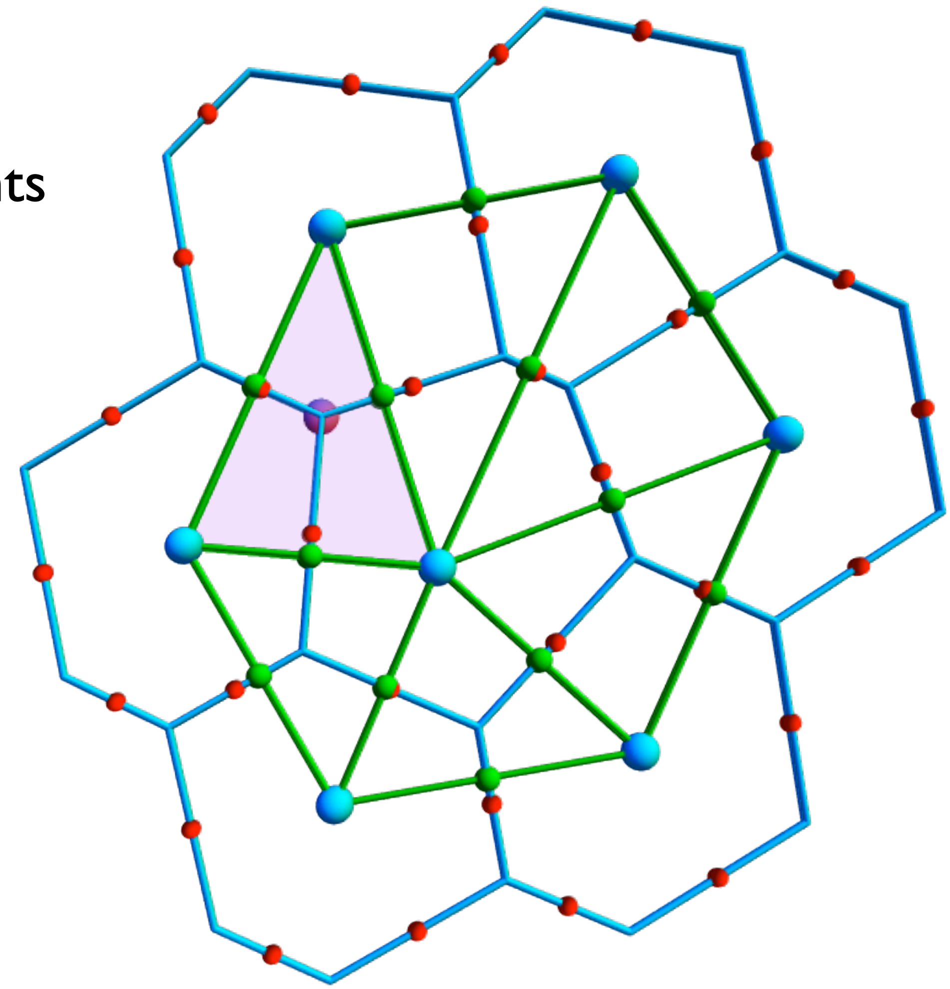

# Grid Optimization Algorithm

- The *goodness* of  particular configuration of points can be expressed as a cost function:

$$F = \sum_{n=1}^{\text{all cells}} \sum_{i=1}^{\text{cell walls}} \left( \text{goodness of wall} \right)_{n,i}^{2}$$

- Solved using quasi-Newton methods:

$$\underset{\mathbf{x}}{\text{minimize}}\, F\left(x_1, x_2, \ldots, x_m\right)$$

- Other grid properties can be optimized using different cost functions

# Grid Optimization Algorithm

- Number of independent variables:
- The number of independent variables (and computer memory) is reduced by using symmetries intrinsic to the grid. Great circles can partition the sphere into 120 triangular subdomains.
- Parallelization of the algorithm
- Many weird problems pop up at higher resolutions

| grid resolution | number of independent variables |
|---|---|
| **(8)** 655,362 (31.27km) | 8,192 |
| **(9)** 2,621,442 (15.64km) | 32,768 |
| **(10)** 10,485,762 (7.819km) | 131,072 |
| **(11)** 41,943,042 (3.909km) | 524,288 |
| **(12)** 167,772,162 (1.955km) | 2,097,152 |

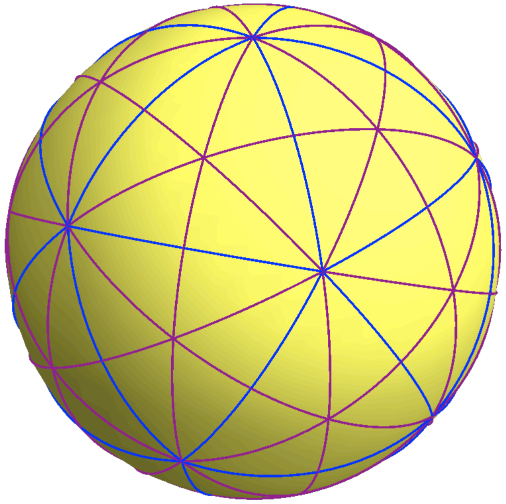

# RMS errors of finite-difference Laplacian and Jacobian

- With a very smooth analytic test function show the convergence properties of the optimized and non-optimized grids

- The RMS error measures the overall goodness of the grid

- The red line shows idealized 2nd-order convergence

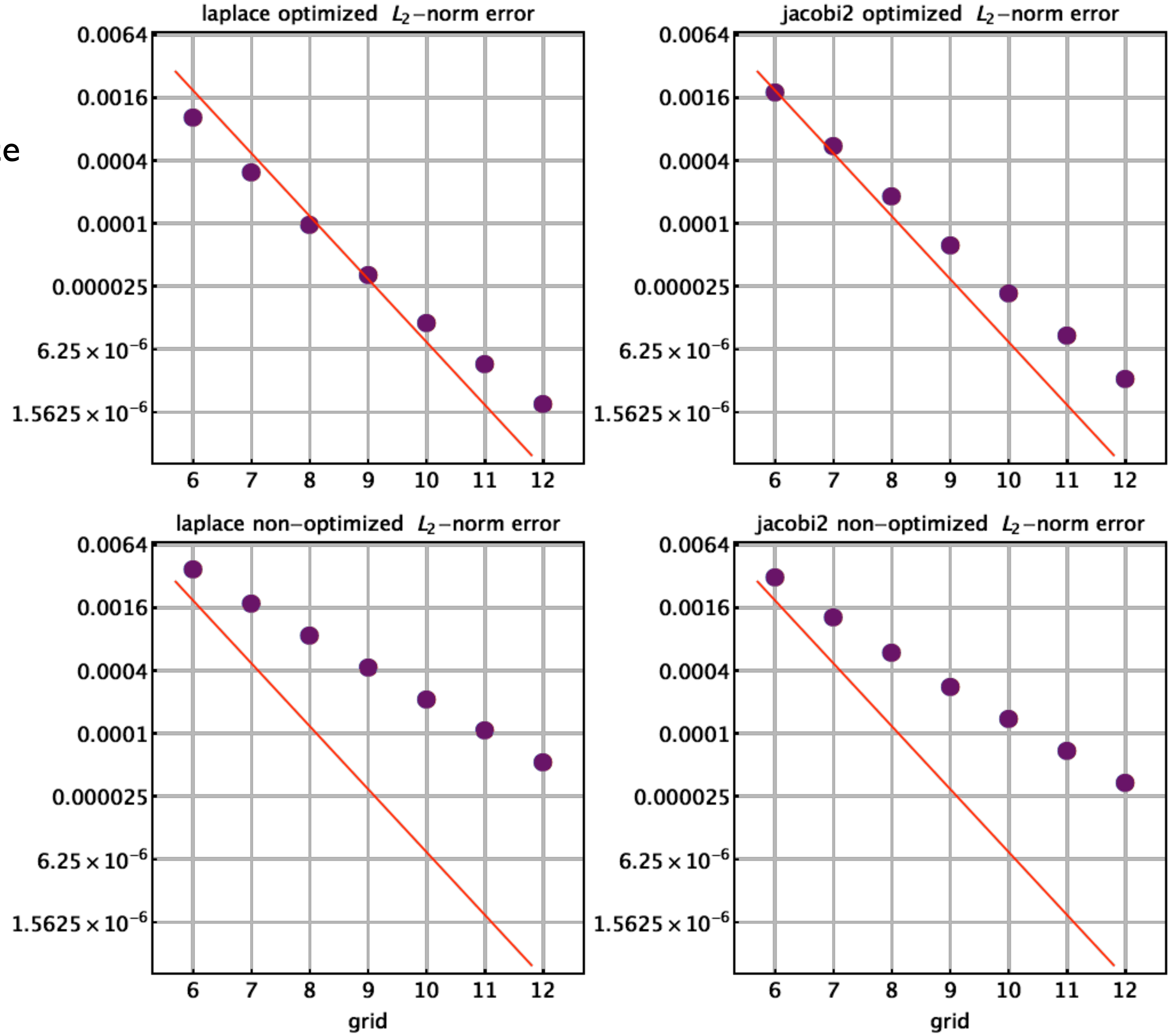

# Maximum errors of finite-difference Laplacian and Jacobian

- With a very smooth analytic test function show the convergence properties of the optimized and non-optimized grids
- The inf-norm error measures the worst case of the grid
- The red line shows idealized 1st-order convergence

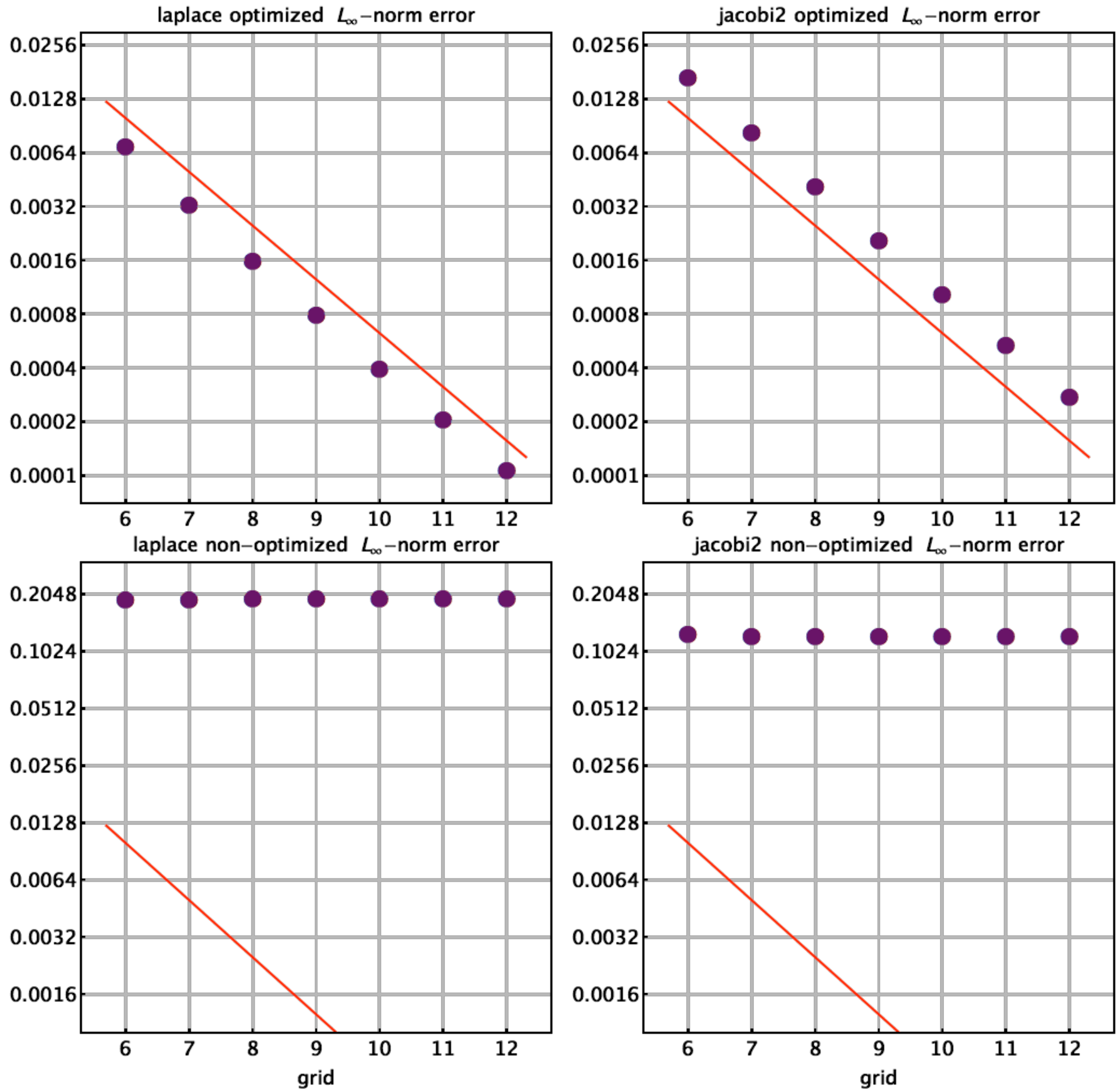

# Possible choices for the global grid

Icosahedral

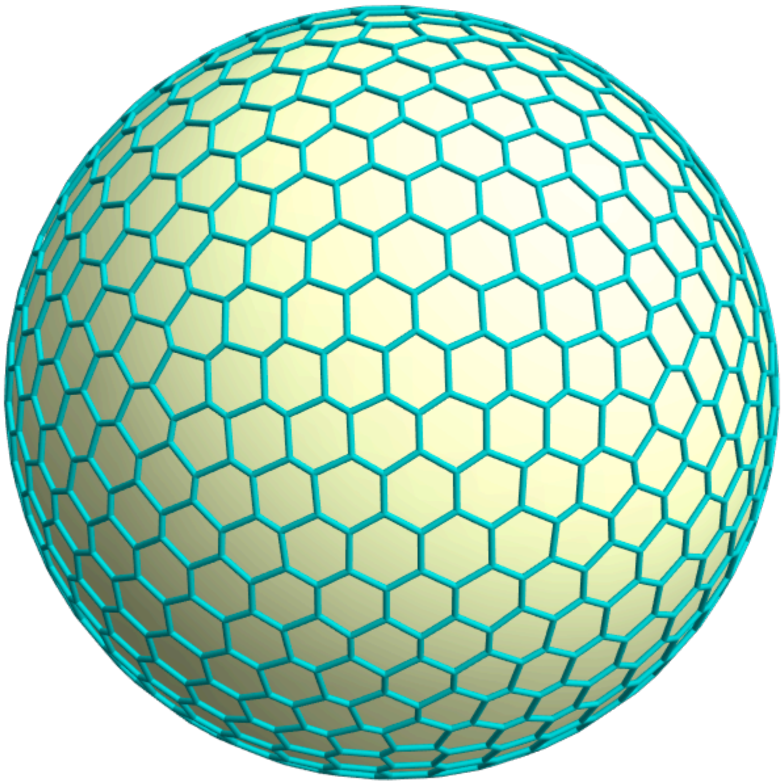

- more isotropy. 6 *directions* associated with each cell center
- more uniformity at panel edges
- maps onto conventional 2D data structure

Cubed Sphere

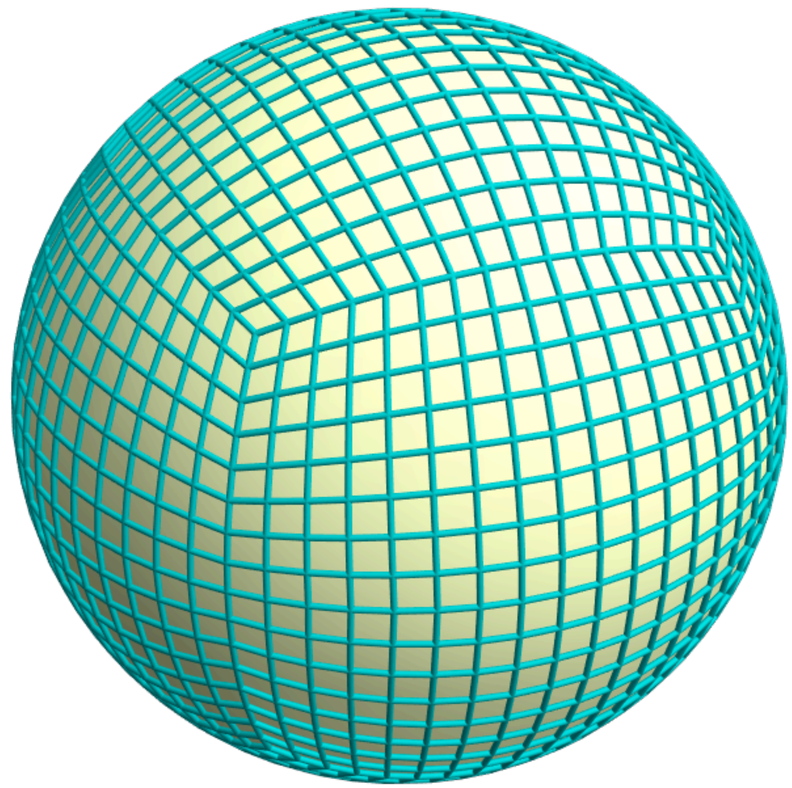

- less isotropy. 4 *directions* associated with each cell center
- less uniformity at panel edges
- maps onto conventional 2D data structure

# Possible choices for staggering variables on the discrete grid

- We use the **Z-grid staggering** of the discrete quantities where vorticity, divergence and potential temperature are defined at cell centers. Does not include a computational mode.
- This can be contrasted with the **C-grid staggering** where momentum is defined normal to cell walls and vorticity is defined at cell corners.
- The C-grid staggering allows a **computational mode.**

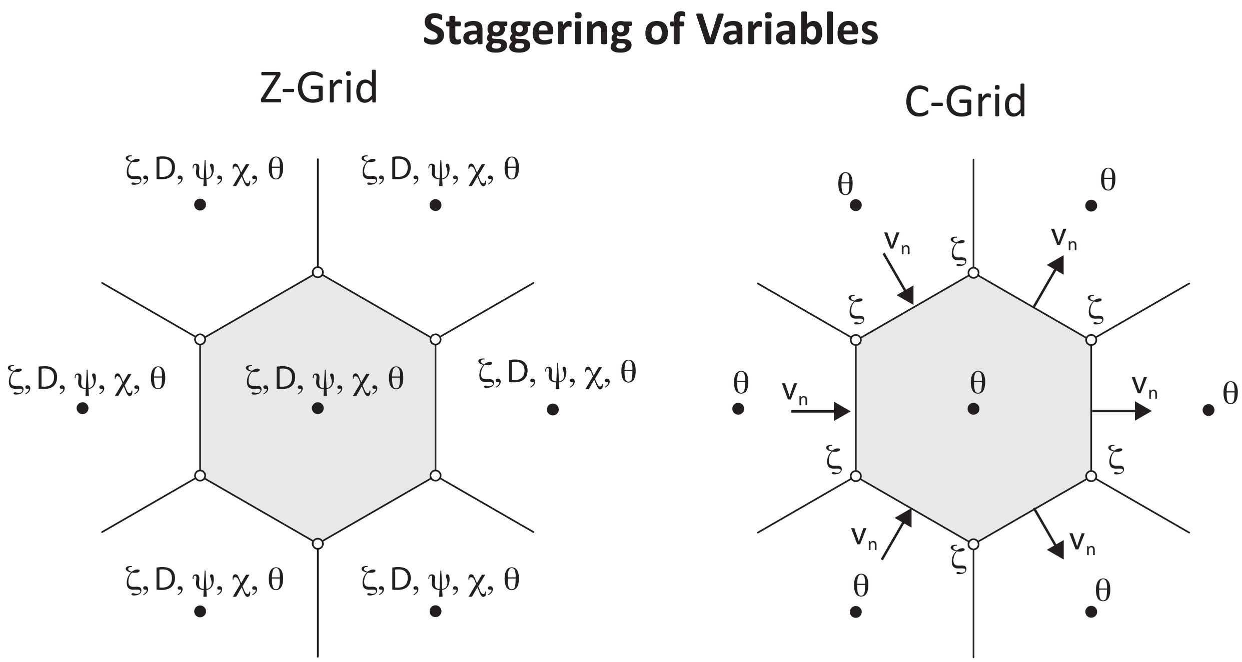

# Model equations of the dynamical core

- Vorticity

$$\frac{\partial \zeta}{\partial t} + \nabla_H \bullet (\zeta_a \mathbf{v}) + \mathbf{k} \bullet \nabla_H \times \left( w \frac{\partial \mathbf{v}}{\partial z} \right) + J(c_p\theta, \pi_{qs}) + J(c_p\theta, \delta\pi) = F_\zeta$$

- Divergence

$$\frac{\partial D}{\partial t} - J(\zeta_a, \chi) - \nabla_H \bullet (\zeta_a \nabla_H \psi) + \nabla_H \bullet \left( w \frac{\partial \mathbf{v}}{\partial z} \right) + \nabla^2 K + \nabla_H \bullet (c_p \theta \nabla_H \pi_{qs}) + \nabla_H \bullet (c_p \theta \nabla_H \delta\pi) = F_D$$

- Potential Temperature

$$\frac{\partial \theta}{\partial t} + \frac{1}{\rho_{qs}} \left[ \nabla_H \bullet (\rho_{qs} \theta \mathbf{v}) - \theta \nabla_H \bullet (\rho_{qs} \mathbf{v}) \right] + \frac{1}{\rho_{qs}} \left[ \frac{\partial}{\partial z} (\rho_{qs} \theta w) - \theta \frac{\partial}{\partial z} (\rho_{qs} w) \right] = \frac{Q}{\pi_{qs}}$$

- Vertical mass flux

$$\frac{\partial}{\partial z} (\rho_{qs} w) = -\boldsymbol{\nabla}_H \bullet (\rho_{qs} \mathbf{v}) - \frac{\partial \rho_{qs}}{\partial t}$$

# Model equations of the dynamical core

- $\rho_{qs}$, $\partial\rho_{qs}/\partial t$ and $\pi_{qs}$ are determined from predicted potential temperature
- $\delta\pi$ is obtained from a 3D elliptic equation

$$\rho_{qs}\boldsymbol{\nabla}_H \bullet \left(c_p\theta\boldsymbol{\nabla}_H\delta\pi\right) + \frac{\partial}{\partial z}\left(\rho_{qs}c_p\theta\frac{\partial}{\partial z}\delta\pi\right)$$

$$= \rho_{qs}A_D + \frac{\partial}{\partial z}A_w - \rho_{qs}\boldsymbol{\nabla}_H \bullet \left(c_p\theta\boldsymbol{\nabla}_H\pi_{qs}\right) + \frac{\partial}{\partial t}\left(\mathbf{v}\bullet\boldsymbol{\nabla}_H\rho_{qs}\right) + D\frac{\partial\rho_{qs}}{\partial t} + \frac{\partial^2\rho_{qs}}{\partial t^2}$$

- Construct a 3D multigrid solver
  - Neumann boundary conditions
  - variable coefficients

# Scaling test of 3D-multigrid on Jaguar XT5

- The **NCCS Cray XT5** with 244,256 cores.
  Each compute node contains two hex-core AMD Opteron processors, 16GB memory, and a SeaStar 2+ router.
- 20 V-cycles
- 128 layers

| Time (s) 128 vertical layers 20 V-cycles | | Number of cores | | | | |
|---|---|---|---|---|---|---|
| | | 5120 | 10240 | 20480 | 40960 | 81920 |
| Grid resolution. Number of cells. (Grid point spacing) | 41,943,042 (3.909km) | 16.867 | 8.971 | 5.590 | 4.004 | |
| | 167,772,162 (1.955km) | 62.527 | 33.978 | 18.057 | 8.746 | 5.066 |
| | 671,088,642 (0.977km) | insufficient memory per core | insufficient memory per core | 62.717 | 32.006 | 17.166 |

# Warm Bubble Test

- Initial condition is the 3D version of Mendez-Nunez and Carroll (1994)
- The initial bubble is 6.6K warmer than the environment.
- The globe is 6.37km in radius (1000×smaller)
- The model's resolution is
  - 163842 cells resulting in 63 m horizontally
  - 160 levels resulting in 75 m vertically

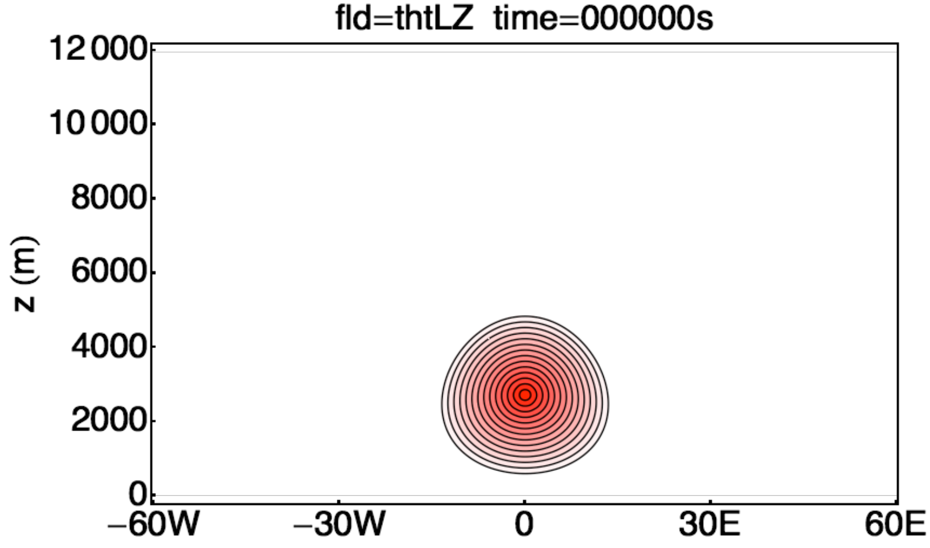


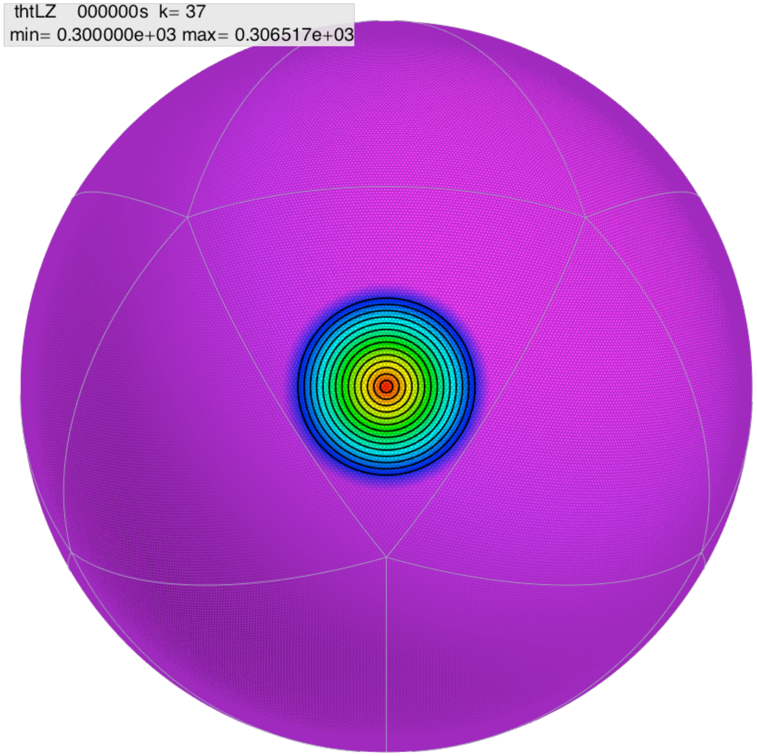

# Warm Bubble Test

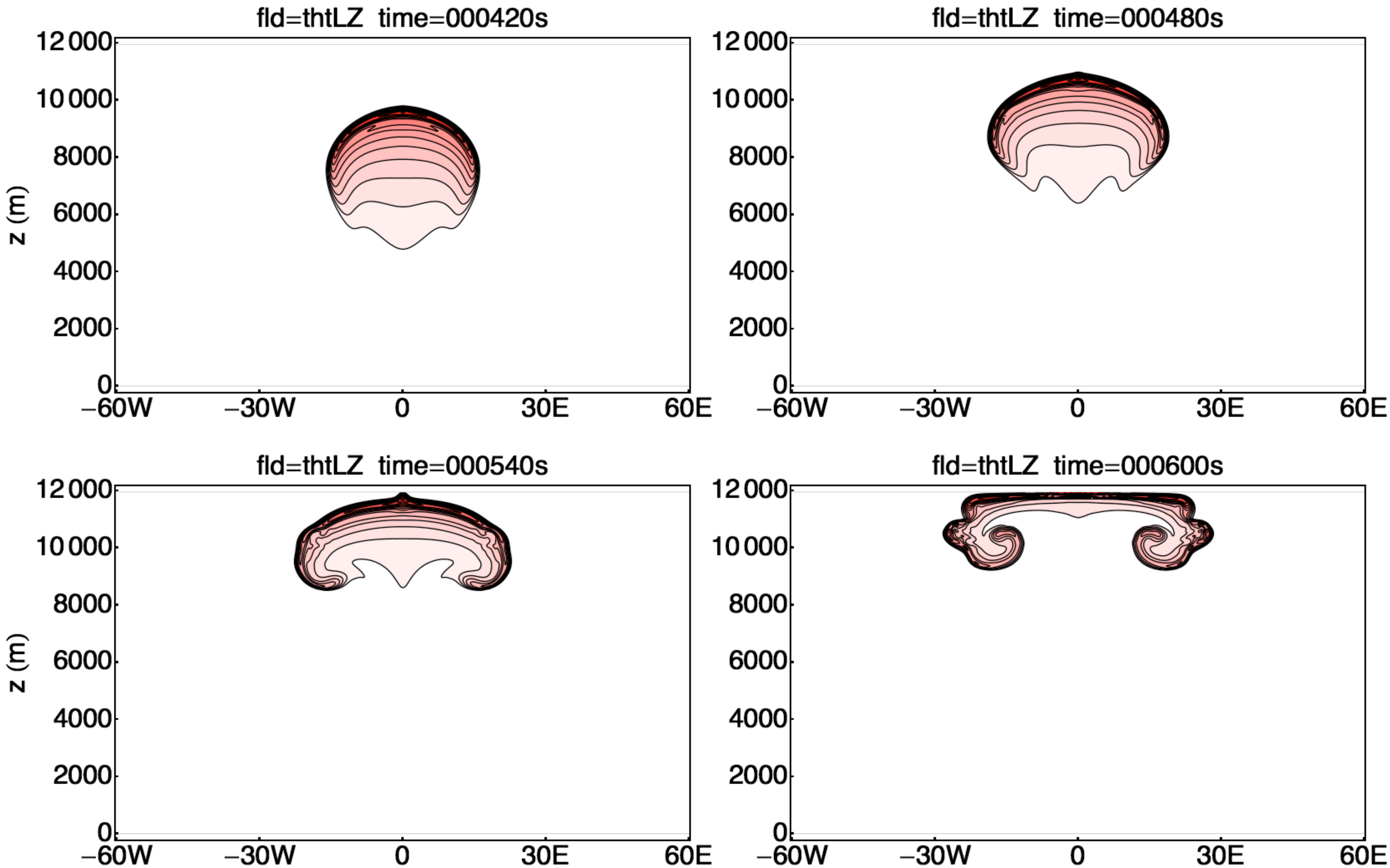

# Extratropical cyclone

- Jablonowski and Williamson (2006) *Quart. J. Roy. Meteor. Soc.*, **132,** 2943-2975
- 40962 cells (125 km). 36 layers.

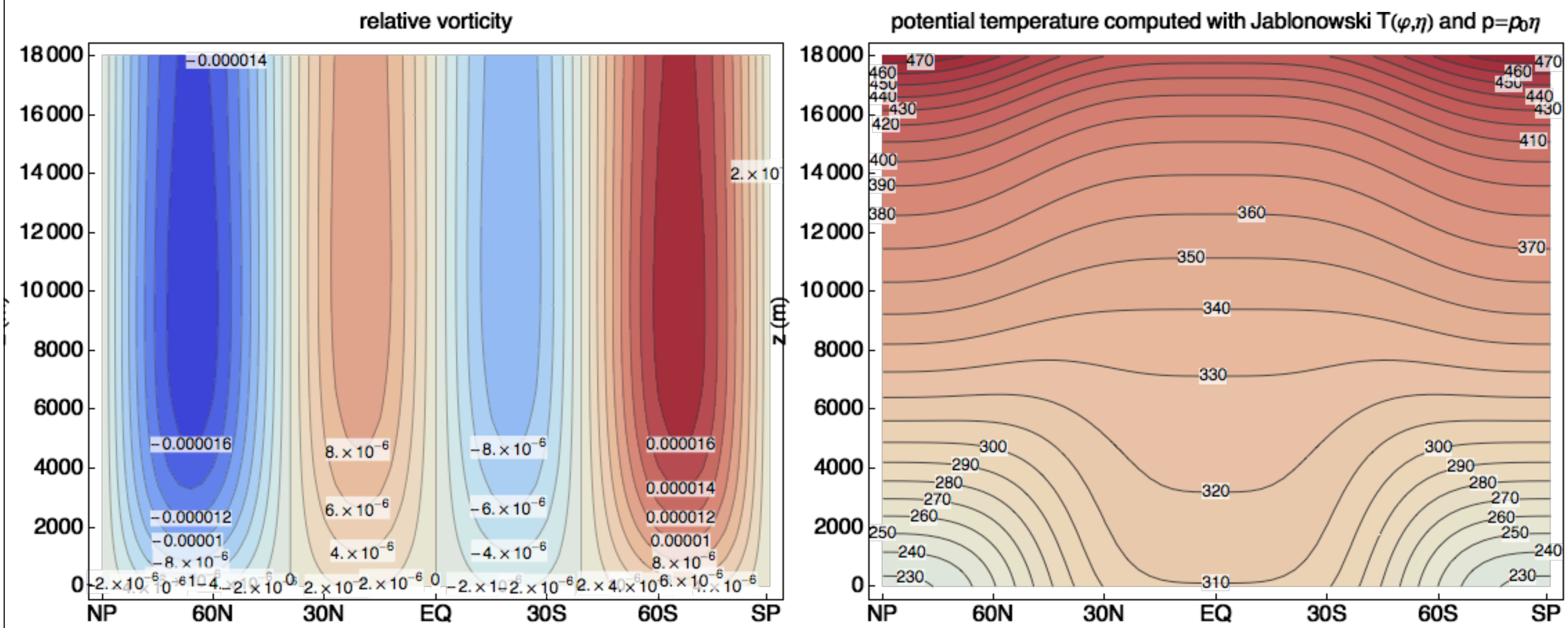

# Extratropical cyclone

- Surface Potential Temperature
- Days 8,9,10 and 11

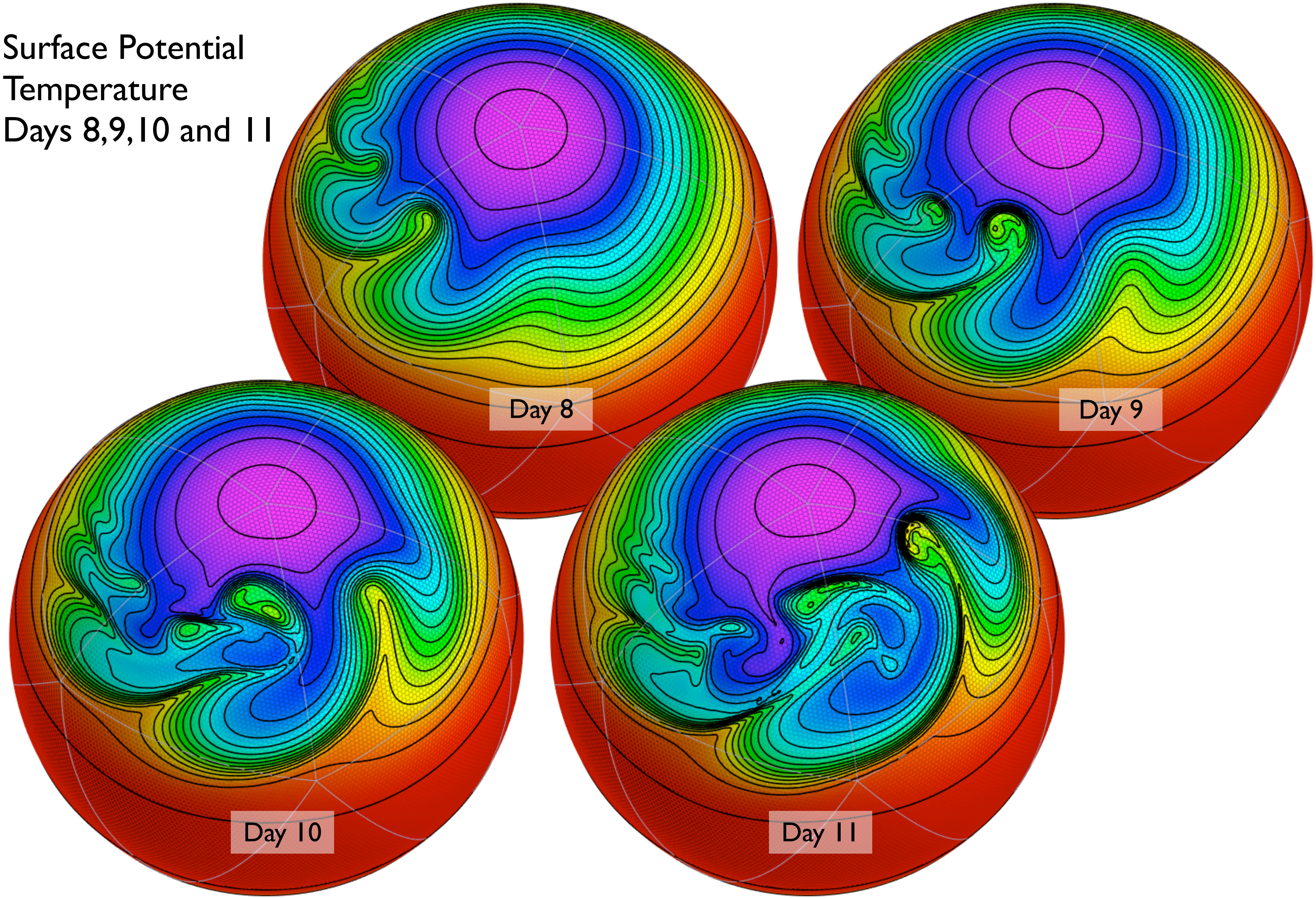

## progress, conclusions and future work

- The grid optimization stuff is finally laid to rest.
- A vorticity-divergence model based on the nonhydrostatic unified system of equations on the icosahedral grid has been developed and tested.
- Addition of physics